$$p_l(+|0) = u_{l+}$$
$$p_l(0|0) = u_{l0}/(z-3) \quad (A.3)$$
$$p_l(-|0) = u_{l-}$$

The two-segment conditional probabilities on the left are defined by eq 31. The terms on the right are defined by FYD as the statistical weights for bonds which are connected to horizontal bonds in layer l. The factor $(z-3)$ is due to indistinguishability of horizontal bond directions. Symmetry conditions, eq 39, permit the other two-segment conditional probabilities defined in eq 31 to be defined in terms of the quantities in eq A.3:

$$p_l(0|+) = u_{l+}p_l(0)/p_{l+1}(-)$$
$$p_l(0|-) = u_{l-}p_l(0)/p_l(-) \quad (A.4)$$

where we have used eq 27 to eliminate $p_{l-1}(+)$. The remaining two conditionals can be constructed by using two of the normalization constraints

$$p_l(-|+) = 1 - (z-2)u_{l+}p_l(0)/p_{l+1}(-)$$
$$p_l(+|-) = 1 - (z-2)u_{l-}p_l(0)/p_l(-) \quad (A.5)$$

The third normalization condition

$$u_{l+} + u_{l0} + u_{l-} = 1 \quad (A.6)$$

is common to the FYD and present treatment. One additional symmetry condition must be satisfied

$$p_l(-|+)p_{l+1}(-) = p_l(+|-)p_{l-1}(+) \quad (A.7)$$

Combination of these results leads to the continuity constraint of FYD (for $h = 1$)

$$p_{l+1}/2 - p_{l-}/2 = q_l(u_{l+} - u_{l-}) \quad (A.8)$$

Thus the constraint conditions of FYD are seen to follow from the symmetry and normalization conditions used in the present treatment. The partition functions differ, however; the consequences are described in the text.

References and Notes

(1) Mandelkern, L. *Faraday Discuss. Chem. Soc.* **1979**, *68*, 310.
(2) Flory, P. J. *J. Am. Chem. Soc.* **1962**, *84*, 2857.
(3) Peterlin, A. *Macromolecules* **1980**, *13*, 777.
(4) *Faraday Discuss. Chem. Soc.* **1979**, 68.
(5) DiMarzio, E. A.; Guttman, C. M. *Polymer* **1980**, *21*, 733.
(6) DiMarzio, E. A.; Guttman, C. M.; Hoffman, J. D. *Polymer* **1980**, *21*, 1379.
(7) Guttman, C. M.; DiMarzio, E. A.; Hoffman, J. D. *Polymer* **1981**, *22*, 1466.
(8) Mansfield, M. L. *Macromolecules* **1983**, *16*, 914.
(9) Flory, P. J.; Yoon, D. Y.; Dill, K. A. *Macromolecules* **1984**, *17*, 862.
(10) Helfand, E. *J. Chem. Phys.* **1975**, *63*, 2192.
(11) Helfand, E. *Macromolecules* **1976**, *9*, 307.
(12) Mullins, W. W. *Phys. Rev.*, **1959**, *114*, 389.
(13) Feller, W. *An Introduction to Probability Theory and Its Applications*; Wiley: New York, 1968; Vol. I.

Molecular Relaxations in Halar, an Alternating Copolymer of Ethylene and Chlorotrifluoroethylene

Yash P. Khanna* and John P. Sibilia

Corporate Technology, Allied Corporation, Morristown, New Jersey 07960

Swayambu Chandrasekaran

Plastics and Engineering Materials Division, Chemical Sector, Morristown, New Jersey 07960. *Received February 17, 1986*

ABSTRACT: Molecular relaxations in Halar, a predominantly alternating 1:1 copolymer of ethylene (E) and chlorotrifluoroethylene (CTFE), have been studied with dynamic mechanical analysis as the primary technique. The mechanisms of the four relaxations, α, β', β'', and γ, occurring over the −130 to +230 °C region have been studied by changing physicochemical variables such as crystallinity, molecular weight, and the degree of alternation. The α-relaxation occurs between +100 and +200 °C and is determined primarily by the crystalline characteristics, i.e., crystallinity, crystallite thickness, and/or crystallite perfection. Motions of the polymer segments at the crystalline–amorphous interface, characterized by a very high activation energy of 129 kcal/mol, are believed to be responsible for the α-relaxation. The onset of the β'-relaxation at 65 °C is identified as the glass transition (T_g) of Halar. The β'-peak occurs at about 85 °C. The β''-relaxation at 50 °C is also an amorphous phenomenon but is believed to involve shorter segments than those responsible for the β'-relaxation or the T_g. A lower activation energy of the β''-process relative to that of the β'-process (66 vs. 107 kcal/mol) supports this assignment. The γ-relaxation occurs at about −55 °C but extends from −120 to +20 °C. Our results suggest that small units of the polymer chain, perhaps 3–4 carbon atoms in length, belonging to various physicochemical environments may be responsible for the γ-peak. Its activation energy, i.e., 27 kcal/mol, is also the lowest of all the relaxations in Halar.

Introduction

Halar is the trademark for Allied Corporation's copolymer products made from ethylene (E) and chlorotrifluoroethylene (CTFE). At present the major application of standard Halar (50E:50CTFE, alternating copolymer) is in the cable-coating industry where this material could be exposed to high temperatures. Accordingly, in a recent study we described the effect of high-temperature aging on the physicochemical characteristics of Halar, including a detailed analysis of the melting behavior.[1,2] Prior to melting, several molecular relaxations occur in polymers at characteristic temperatures which dictate the product applicability. Earlier we had reported a study of these molecular relaxations[3] in Halar in the −100 to +200 °C region based on mechanical spectra. Since then we have learned more about the phenomenon of molecular motions in Halar over the temperature range −130 to +230 °C, and this is the subject of the present paper.

Experimental Section

Materials. The samples selected for this study are listed in Table I. Halar 300 and Halar 500 differ only in molecular weight

0024-9297/86/2219-2426$01.50/0

Table I
Transitions in Halar: Differential Scanning Calorimetry and Thermomechanical Analysis

sample description							DSC		TMA
no.	type	thermal history	composition E:CTFE	$[\eta]$, dL/g	crystallinity, %	density, g/cm^3	T_m, °C	ΔH_f, cal/g	penetration temp, T_g, °C
1	Halar 300	slow-cooled	1:1		43	1.684	242	9.5	
2		quick-quenched	1:1		30	1.671	242	8.5	
3		standard	1:1	0.80	38	1.678	243	9.4	48
4		at 200 °C/100 h	1:1		44	1.690	230 and 242	10.7	
5	Halar 500	standard	1:1	0.49	47	1.690	241	10.0	51
6	Halar polymerized at −78 °C	standard	1:1	0.14	37	1.696	257	11.3	56
7		quick-quenched	1:1		35	1.685	261	10.6	56
8	Halar polymerized at +60 °C	standard	1:1	0.97	36	1.704	232	6.7	54
9	Halar 6000	standard	1:1 with 2.5% HFIB		28	1.678	230	7.3	
10		standard	1:1 with 6.0% HFIB		27	1.668	213	5.0	

and both are commercially available, 1:1 copolymers of E/CTFE with about 85% alternating (crystallizable) units; the remaining units consist of noncrystallizable short blocks of E and CTFE. Experimental Halars polymerized at −78 and +60 °C have a degree of alternation higher and lower than 85%, respectively. Halar 6000 samples are terpolymers of E, CTFE, and hexafluoroisobutylene (HFIB), with the crystallizing units consisting of alternating E/CTFE sequences.

Sample Preparation. Square plaques measuring 2 in. × 2 in. and about 50-mil thickness were molded. Sample 1 was molded and then slow-cooled in the molding press by turning off the power whereas sample 2 was quick-quenched in ice/water. All other samples were molded under standard conditions, i.e., cooled in air after the molding. A portion of sample 3, i.e., Halar 300 molded under standard conditions, was also annealed in air for 100 h at 200 °C (sample 4). All the experimental work was carried out on the molded samples.

Density. Density measurements were made at 23 °C by using the ASTM D-1505 density gradient method. Data reported are the average of triplicate measurements.

Viscosity. Intrinsic viscosity $[\eta]$ of the polymers was measured at 135 °C with a Cannon-Ubbelohde viscometer. The solutions were prepared by dissolving the polymers in 2,5-dichlorobenzotrifluoride at 160 °C for 2 h. A slightly higher temperature was necessary to dissolve the Halar polymerized at −78 °C.

X-ray Diffraction. X-ray diffraction (XRD) patterns were recorded on a Phillips APD 3600 automated system in the parafocus mode using Cu Kα radiation. Crystalline index was obtained by measuring the area under the reflection at $2\theta = 18.2°$ and the total area of the crystalline and amorphous scattering. In order to obtain the crystallinity that best represented a particular sample, multiple measurements were made on both sides of the molded piece and the average crystallinity value was taken.

Differential Scanning Calorimetry (DSC). A Perkin-Elmer DSC-2 interfaced with a 3600 data station was used for measuring the melting temperature (T_m) and the heat of fusion (ΔH_f). A sample of about 10 mg was crimped in an Al pan and heated at 10 °C/min in an argon atmosphere. Specific heat (C_p) was also measured as a function of temperature (triplicate analysis) for Halar 300, using a sample size of about 35 mg and a heating rate of 5 °C/min.

Thermomechanical Analysis (TMA). A Perkin-Elmer TMS-2 interfaced with a 3600 data station was used in the penetration mode (20-g load) as well as in the expansion mode (no load). The samples were heated in a helium atmosphere at 10 and 5 °C/min for the penetration and expansion modes, respectively.

Dynamic Mechanical Analysis (DMA). A Polymer Laboratories DMTA unit attached to a Hewlett-Packard 9836 computer was used in obtaining the mechanical spectra. A sample of approximately 4-cm length, 1-cm width, and 0.125-cm thickness was analyzed in the bending mode of deformation at a heating rate of 3 °C/min from −130 to about +230 °C under an argon atmosphere. All the samples were analyzed at a constant frequency of 1 Hz and a constant strain level, and the unit was operated in the double-cantilever mode.

A sample of Halar 300 (quick-quenched) was also studied for the effect of frequency ranging from 0.1 to 30 Hz.

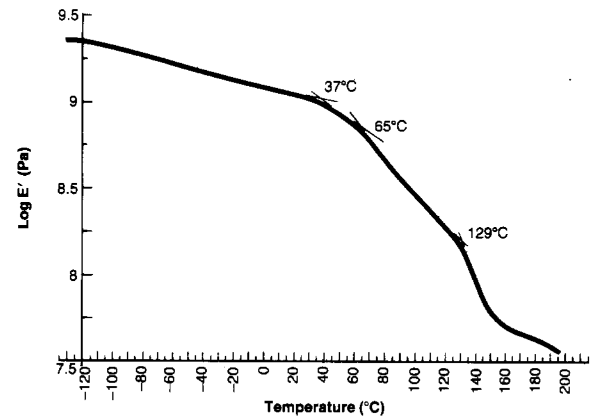

Figure 1. Dynamic storage modulus (E') vs. temperature for Halar 300.

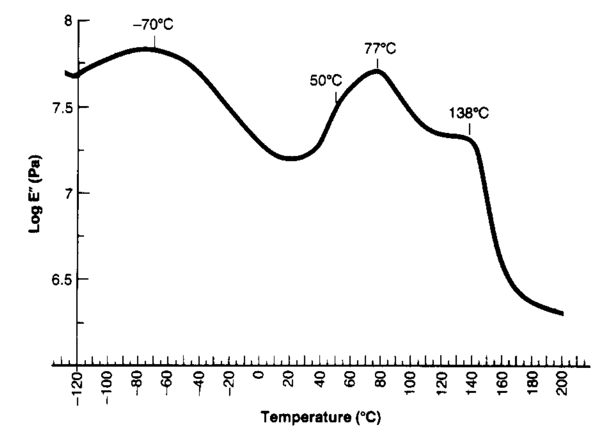

Figure 2. Dynamic loss modulus (E'') vs. temperature for Halar 300.

Results and Discussion

Typical plots of temperature-dependent dynamic storage modulus (E'), dynamic loss modulus (E''), and damping factor ($\tan \delta = E''/E'$) are shown in Figures 1, 2, , and 3, respectively. In this paper discussion of the relaxation phenomenon is made mostly on the basis of $\tan \delta$ peaks. As shown in Figure 3, four molecular relaxations, i.e., α, β', β'', and γ, occur in Halar over the temperature range −130 to +230 °C (Tables I–III).

α-Relaxation. The α-peak varies from +100 to +200 °C for the studied Halar compositions. We propose a model for the α-relaxation process based on the following:

(1) Relaxation Strength Analysis. It is well documented that in dynamic mechanical analysis, the intensity of an amorphous relaxation increases with an increase in amorphous fraction.[4,5] Similarly, the intensity of a crys-

Table II
Transitions in Halar: Dynamic Mechanical Analysis

sample no.	α-relaxation (tan δ basis) temp, °C	α-relaxation (tan δ basis) intensity	β′-relaxation: E′ basis onset temp, °C	β′-relaxation: tan δ basis peak temp, °C	β′-relaxation: tan δ basis peak intensity	β″-relaxation: E′ basis onset temp, °C	β″-relaxation: E′ basis Δ log E′	β″-relaxation: peak temp, °C	γ-relaxation, (tan δ basis) peak temp, °C	γ-relaxation, (tan δ basis) peak intensity
1	155, 155, 155	0.165, 0.165, 0.165	66, 67, 67	87, 88, 88	0.085, 0.085, 0.085	31, 33, 35	0.17, 0.17, 0.17	50	−54	0.019
2	130	0.199	65	90	0.131	30	0.20	50	−56	0.019
3	144, 143, 142 } 143	0.202, 0.190, 0.213 } 0.202	65, 65, 62 } 64	88, 85, 80 } 84	0.103, 0.106, 0.108 } 0.106	37, 36, 35 } 36	0.19, 0.14, 0.21 } 0.18	54, 55, ? } 55	−55	0.018
4	150	0.239	72	90	0.089	37	0.13		−52	0.017
5	142	0.215	62, 65 } 64	81, 82 } 82	0.108, 0.116 } 0.112	36, 32 } 34	0.20, 0.20 } 0.20	?, 45 } 45	−51	0.020
6	∼200	∼0.210	72, 72, 70 } 71	100, 105, 95 } 100	0.108, 0.120, 0.110 } 0.113	30, 30, 38 } 33	0.14, 0.11, 0.07 } 0.11	50, ?, 48 } 49	−50	0.018
7	172	0.165	70, 70 } 70	92, 92 } 92	0.130, 0.127 } 0.129	30	0.13	52	−63	0.013
8	124, 125 } 125	0.187, 0.190 } 0.189	64, 66 } 65	82, 82 } 82	0.125, 0.127 } 0.126	33, 38 } 32	0.17, 0.07 } 0.17	?, ?	−50	0.018
9	118, 113 } 116	0.232, 0.230 } 0.231	68, 63 } 66	85, 80 } 82	0.171, 0.156 } 0.164				−54	0.021
10	110, 106 } 108	0.216, 0.220 } 0.218	68, 65 } 67	83, 78 } 81	0.225, 0.215 } 0.220				−52	0.020

Table III
Transitions in Halar: Relaxation Strength Analysis

sample no.	crystallinity, %	Δ log E′ for the relaxations: α	Δ log E′ for the relaxations: β′ + β″	Δ log E′ for the relaxations: α + (β′ + β″)	Δ log E′ for α + (β′ + β″) relaxations calcd for 100% amorphous sample
1	43	0.74, 0.73 } 0.74	0.64, 0.63 } 0.64	1.38, 1.36 } 1.37	2.4
2	30	0.71	0.67	1.38	2.0
3	38	0.72, 0.68, 0.73 } 0.71	0.71, 0.55, 0.67 } 0.64	1.43, 1.23, 1.40 } 1.35	2.2
4	44	0.77	0.54	1.30	2.3
9	28	0.73, 0.72 } 0.73	0.80, 0.74 } 0.77	1.53, 1.46 } 1.50	2.1
10	27	0.77	0.99	1.76	2.4

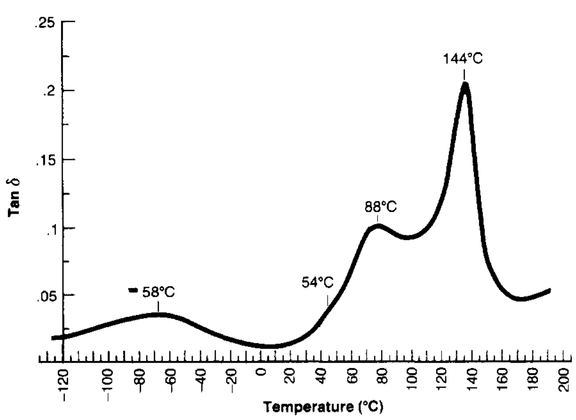

Figure 3. Damping factor [tan δ (E''/E')] vs. temperature for Halar 300.

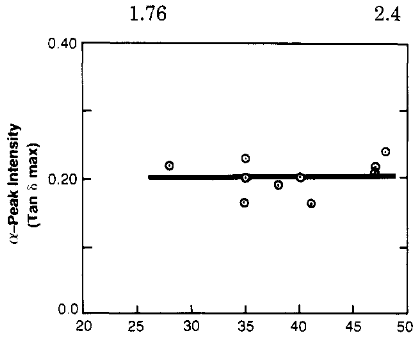

Figure 4. Relationship between α-relaxation intensity and the crystallinity of Halar.

talline relaxation must increase with increasing crystallinity. Now the question is what criterion, i.e., E', E'', or tan δ, for intensity would best represent the origin of a particular relaxation. In a recent review, Boyd[6] suggests the use of tan δ as an index of phase origin.

In Figure 4, α-peak intensity (tan δ basis) has been plotted against crystallinity. It is apparent that the amount of crystallinity has no influence on the intensity of α-relaxation. Similar information is revealed when evaluating the relaxation strength on the basis of E'; e.g., Δ log E' across the α-relaxation is constant at 0.74 (±0.03)

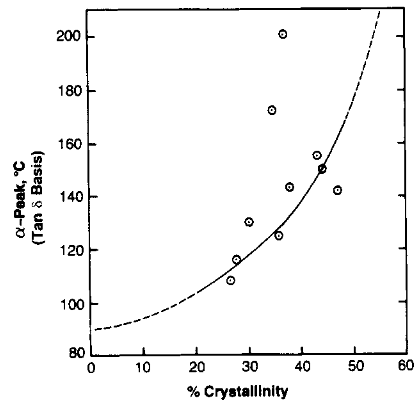

Figure 5. Relationship between α-relaxation temperature and the crystallinity of Halar.

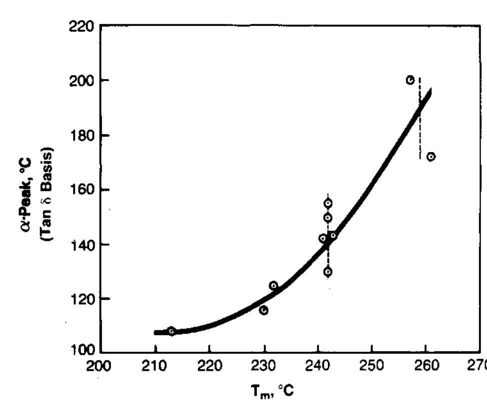

Figure 6. Relationship between α-relaxation temperature and the melting temperature of Halar.

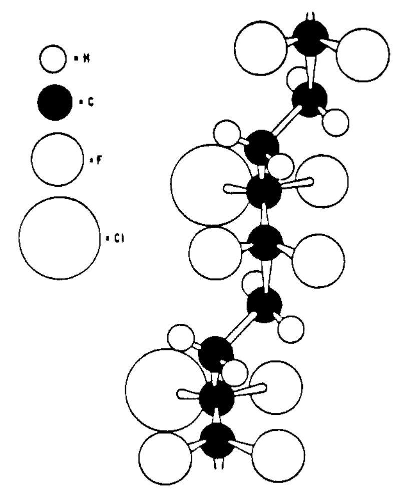

Figure 7. Kinked structure of the 1/1 alternating Halar.

regardless of the crystallinity (Table III).

Our experience with several amorphous polymers has shown that the $\Delta \log E'$ across the T_g is 2.3–2.5. If we consider the α-, β'-, and β''-relaxations to be all associated with the amorphous phase, then the total $\Delta \log E'$ calculated for the 100% amorphous sample becomes 2.0–2.4 (Table III). In other words, in the absence of crystallinity, the total $\Delta \log E'$ for the α-, β'-, and b″-relaxations is typically what one expects for an amorphous polymer. Therefore, indirectly we are attributing the α-relaxation to an amorphous phenomenon. As the following sections will show, the α-process involves the motion not of the discrete amorphous phase but of the interfacial amorphous regions (tie molecules, folds, loops, etc.). The following may be reasons why the α-relaxation strength does not increase with increasing amorphous content: (a) Due to experimental difficulties, the amorphous content in Halar could not be widened more than 53–73% so as to get a clearer picture of the phase origin of the α-relaxation, and (b) coincidentally, the amount of interfacial amorphous phase may be the same in samples showing a crystallinity range of 27–47%.

(2) Influence of Crystallinity. Although the intensity of the α-relaxation remains unaffected by crystallinity, its temperature increases with increasing crystalline content (Figure 5). At high crystallinities (e.g., >50%), the α-peak will occur at temperatures above 200 °C and thus will be masked by the melting process. The data in Figure 5 extrapolated to zero crystallinity suggest that an amorphous Halar would exhibit the α-peak at 90 °C; the latter interestingly coincides with the T_g of Halar. We are suggesting that the α-peak temperature increases with increase in crystallinity as well as crystallite thickness and/or crystallite perfection; by crystallite thickness we imply lamellae thickness or fold length. An interplay of these factors can very well be responsible for the scattered data points in Figure 5. Although we are unable to separate the contribution of crystallinity alone on the α-relaxation temperature, the influence of crystallinity on the α-relaxation temperature is a reasonable assumption.

(3) Influence of Crystallite Thickness/Crystallite Perfection. The α-relaxation temperature also increases with the increase in melting temperature (T_m) of the Halar crystals (Figure 6). On the basis of the heating rate study,[2] we had shown earlier that the thermal history did not influence the main T_m of Halar. Thus, in Figure 6 a range of α-peaks has been indicated (vertical dashed line) corresponding to various crystallinities obtained by thermal history variations of a particular Halar although the T_m is constant.

For the crystals of a particular polymer, the T_m is primarily related to the crystallite thickness. However, depending upon the polymer, secondary factors such as the nature of the lamellar surface and crystalline defects can also affect the melting temperature. In view of the present and previously reported heating rate study,[2] the possibility of any significant crystal thickening or perfection during the DSC analysis has been ruled out. Thus, the T_m data reflect the crystallite thickness and/or crystallite perfection of the original crystals and not of the crystals reorganized during the DSC analysis. The crystallite thickness of samples 1–3 (Table I) revealed by transmission electron microscopy varies from 90 to 150 Å although their T_m is constant. It is speculated that these samples differ in crystallite perfection. Since we are unable to define better the role of crystallite perfection at present, we are using the T_m data to reflect the overall crystallite thickness and perfection.

Now since the α-relaxation temperature increases with the increase in T_m, it is reasonable to propose that the α-peak temperature increases with an increase in crystallite thickness and/or crystallite perfection.

(4) Motions within Halar Crystals. Our previous work[3,7] has indicated that the preferred conformation of the Halar involves a "kinked" structure in which the CH_2 units are at an angle of about 45° to the molecular axis (Figure 7). Also in the crystalline phase, the adjacent kinked chains are arranged such that the ethylene groups (CH_2CH_2) line up opposite to the chlorotrifluoroethylene ($CClFCF_2$) groups.

In order to understand the origin of the α-relaxation, we had earlier evaluated the infrared dichroic ratios of the four bands related to CH_2 groups as a function of temperature.[3] It was apparent that during the α-relaxation temperature region, a change in the orientation of the CH_2

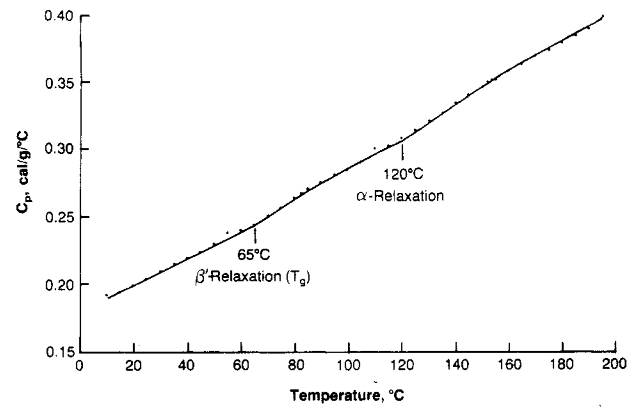

Figure 8. Specific heat (C_p) vs. temperature for Halar 300.

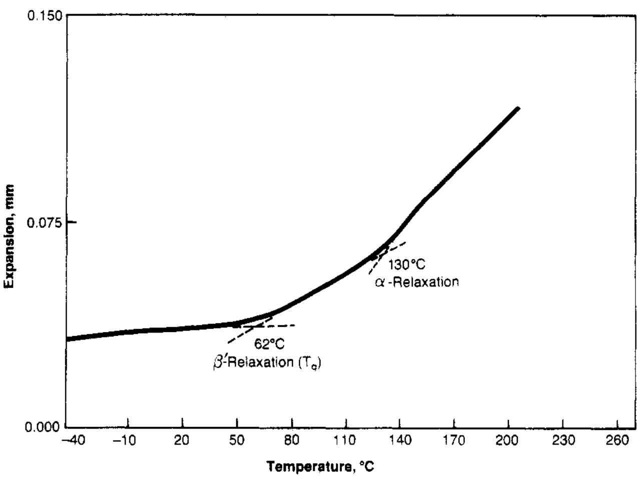

Figure 9. Thermomechanical analysis of Halar 300.

groups had occurred. These results suggested that the plane of the CH_2 groups was aligning with the molecular axis during the α-relaxation. On the basis of this, the α-peak was attributed to a "kinking" to "unkinking" transition.

In complying with all the information described above, we propose a mechanism for the α-relaxation that involves motions of the interfacial amorphous regions. This mechanism is consistent with our results; for example:

(i) The $\Delta \log E'$ calculated for 100% amorphous Halar can only be explained if the α-relaxation is considered as an amorphous process.

(ii) Increase in crystallinity will reinforce the interfacial region so that a higher temperature will be needed for the relaxation to occur (Figure 5). As the crystallinity approaches zero, the relaxation temperature corresponds to that of the amorphous material and interestingly coincides with the T_g of Halar (Figure 5), which occurs at 85 ± 5 °C on the tan δ curve.

(iii) An increase in crystallite thickness and/or crystallite perfection increases the crystalline relaxation temperature. This is shown to occur, for example, in the case of polyethylene.[5] As the crystallite thickness increases, the temperature of the crystal motions increases accordingly. We believe that the crystal motion is a prerequisite for the interfacial region (tie molecules, folds, loops, etc.) to be mobile.[5]

(iv) The onset of the α-relaxation for sample 3, i.e., Halar 300 molded under standard conditions, is about 127 °C by DMA, which compares very well with the onset of specific heat (C_p) increase at 120 °C by DSC (Figure 8). A step increase in C_p at 120 °C, i.e., above the T_g, must reflect the additive contribution of motions from another phase,

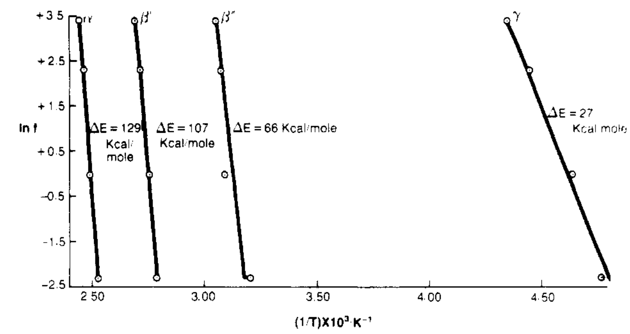

Figure 10. Energy of activation (ΔE) for the molecular relaxations in Halar 300.

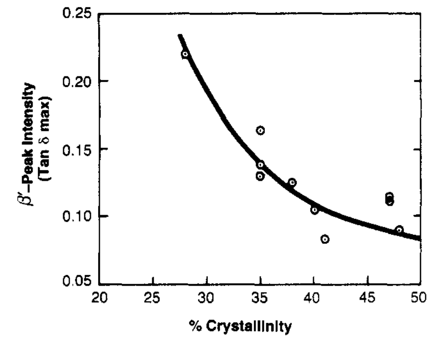

Figure 11. Relationship between β'-relaxation intensity and the crystallinity of Halar.

e.g., interfacial regions. TMA of Halar 300 also indicates an additional increase in linear expansion coefficient at 130 °C, which coincides with the onset of the α-relaxation (Figure 9).

(v) A very high activation energy for the α-relaxation (ΔE = 129 kcal/mol) suggests that it is associated with motions of the relatively rigid amorphous segments (Figure 10). For amorphous relaxations,[8] ΔE normally ranges from 50 to 100 kcal/mol.

(vi) As a precursor of the α-relaxation, the chains in the crystalline regions go from a "kinked" structure to a less "kinked" one.

Earlier reported work[9] based on Raman longitudinal acoustic mode (LAM) experiments suggests that the α-relaxation in Halar involves motions of the phase boundaries. This is consistent with all our results on the α-relaxation process.

β-Relaxation. Two β-peaks occur as a doublet on the DMA thermograms. On the tan δ basis, β' is observed mostly at 85 ± 5 °C (Table II) while β'' is shown at 50 ± 5 °C (Table II). On a comparative basis, β' is by far the more intense transition (Figure 3).

The intensity of the β'-relaxation decreases as the crystallinity increases (Figure 11), thereby suggesting it to be an amorphous phenomenon. The onset of the β'-relaxation by DMA is at 65 ± 5 °C (Figure 1), which is in excellent agreement with the onset temperature of the glass transition at 65 °C by DSC (Figure 8) and with the increased expansion coefficient due to the T_g at 62 °C by TMA (Figure 9). TMA experiments in the penetration mode (Table I) indicate a somewhat lower T_g of 52 ± 4 °C, which probably is due to the load on the penetration probe (note: a load of 20 g was necessary to observe penetration of the probe into the sample). On the basis of our results we suggest that the onset of the β'-relaxation at 65 °C is analogous to the T_g.

The β''-relaxation is a very small transition compared to the β'-relaxation. The β''-relaxation is clearly observed on the dynamic storage modulus, E', curve rather than tan

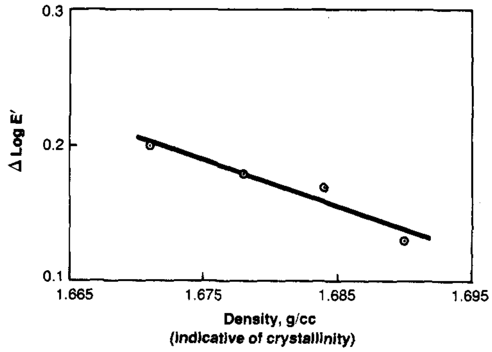

Figure 12. Change in dynamic storage modulus ($\Delta \log E'$) associated with the β''-relaxation as a function of density for Halar 300.

δ curve. Quantitative evaluation of the β''-transition based on the E' data reveals that this is also an amorphous phenomenon (Figure 12). It is known that many polymers exhibit a β-transition below the T_g at a temperature such that $T_\beta/T_g \simeq 0.75$.[10] Also it has been suggested that the β-peak at $0.75T_g$ represents the motions of short amorphous segments. Considering the β'-relaxation as the T_g of Halar, the ratio β''/T_g is about 0.83. Therefore, we believe that the β''-relaxation involves the small-scale or local motion of the amorphous segments of Halar.

To conclude our view on the β-relaxation(s) in Halar, we propose that the β'-peak at 85 ± 5 °C is the T_g of Halar whereas the β''-peak at 50 ± 5 °C is due to the motion of short amorphous segments. Activation energies of 107 and 66 kcal/mol for the β'- and β''-relaxations, respectively, support that these represent large- and small-scale motions of the amorphous regions.

γ-Relaxation. The γ-peak occurs as a very broad peak extending from −120 to +20 C, with the maximum at about −55 °C (Figure 3 and Table II). Its peak intensity remains more or less unaffected by the crystalline (or amorphous) content (Table II).

The lowest temperature relaxations in mechanical spectra have generally been attributed to the motions of the small units of the polymer chain, perhaps 3–4 carbon atoms in length.[5,10,11] The small units in Halar responsible for the α-peak probably comprise (a) short blocks of ethylene (CH_2), (b) short blocks of chlorotrifluoroethylene ($CClFCF_2$), (c) short segments of amorphous 1/1 alternating copolymer, i.e., Halar, and (d) loose chain ends within the amorphous and crystalline phases of Halar. A range of physicochemical environments of the units involved is most likely responsible for the extreme broadness of the γ-relaxation. Comparatively, a low value of the activation energy of the γ-peak (27 kcal/mol) is in agreement with the assignment that it is related to the motions of very small units of the polymer.

Acknowledgment. We thank Mrs. A. Reimschuessel and Prof. S. Krimm for helpful comments and suggestions. Also we acknowledge the contributions of T. Taylor and the late D. Richardson for thermal analysis, S. Murthy, A. Szollosi, and H. Minor for X-ray diffraction, N. Buik for density measurements, and F. Cilurso for viscosity data. We also thank B. Buckner for his high-quality mold-processing work.

Registry No. Halar, 25101-45-5; (E)·(CTFE)·(HFIB) (copolymer), 67124-01-0.

References and Notes

(1) Khanna, Y. P.; Turi, E. A.; Sibilia, J. P.; Sacks, W. *J. Appl. Polym. Sci.* **1984**, *29*, 3607.
(2) Khanna, Y. P.; Turi, E. A.; Sibilia, J. P. *J. Polym. Sci., Polym. Phys. Ed.* **1984**, *22*, 2175.
(3) Sibilia, J. P.; Schaffhauser, R. J.; Roldan, L. G. *J. Polym. Sci., Polym. Phys. Ed.* **1976**, *14*, 1021.
(4) Starkweather, H. W., Jr. *J. Polym. Sci., Polym. Phys. Ed.* **1973**, *11*, 587.
(5) Khanna, Y. P.; Turi, E. A.; Taylor, T. J.; Vickroy, V. V.; Abbott, R. F. *Macromolecules* **1985**, *18*, 1302.
(6) Boyd, R. H. *Polymer* **1985**, *26*, 323.
(7) Sibilia, J. P.; Roldan, L. G.; Chandrasekaran *J. Polym. Sci., Polym. Phys. Ed.* **1972**, *10*(3), 549.
(8) Starkweather, H. W., Jr. *Macromolecules* **1981**, *14*, 1277.
(9) Rabolt, J. F. *Polymer* **1981**, *22*, 890.
(10) McCrum, N. G. In *Molecular Basis of Transitions and Relaxations*; Meier, D. J., Ed.; Gordon and Breach: New York, 1978.
(11) Khanna, Y. P. *J. Therm. Anal.* **1985**, *30*, 153.

Field-Induced Textures and Elastic Constants of Nematic Polymers†

Curtis R. Fincher, Jr.

Central Research and Development Department, Experimental Station, E. I. du Pont de Nemours and Company, Wilmington, Delaware 19898. *Received February 19, 1986*

ABSTRACT: Studies of the development of periodic textures or patterns in a nematic liquid crystalline polymer when a magnetic field is applied orthogonal to the director of the sample are presented. The strong anisotropy of the light scattering from this polymer allows for a clear definition of the obtained texture. While the patterns can be explained by earlier theories for small-molecule nematics, one must assume the existence of a strongly anchored director, contrary to fact.

In recent years there has been considerable effort spent in the investigation of the physics of liquid crystals and more recently an expanding effort in polymers. These two fields share not only many analogies but also a whole class of materials commonly referred to as liquid crystalline polymers (LCP's).[1] LCP's are commonly found in biological systems (generally cholesteric) but have also been found to be technologically important in terms of high-performance materials.[2] In spite of the driving forces of science and technology many of the fundamental properties of these materials are relatively unexplored. The problems have not been due to a lack of interest but rather because many of the standard approaches and techniques which have been developed during the extensive work on small-molecule nematics experience difficulties when applied to investigations of polymeric nematics. As an example, to make most measurements on a nematic mean-

† Contribution No. 3731.

0024-9297/86/2219-2431$01.50/0